

Article

The Direct Synthesis of Aromatic Hydrocarbons from Syngas over Bifunctional MgZrO_x/HZSM-5 Catalysts

Dong Ma, Laizhi Sun ^{*}, Lei Chen, Shuangxia Yang, Xinping Xie, Hongyu Si, Baofeng Zhao  and Dongliang Hua

Energy Research Institute, Qilu University of Technology (Shandong Academy of Sciences), Shandong Provincial Key Laboratory of Biomass Gasification Technology, Jinan 250014, China

* Correspondence: sunlz@sderi.cn; Tel.: +86-0531-82605584

Abstract: ZrO₂ and catalysts were prepared by a co-precipitate method and coupled with a HZSM-5 zeolite catalyst through a mechanical mixing method; these were applied to the direct synthesis of aromatic hydrocarbons from syngas through an oxygen-containing intermediate route. The physical and chemical properties of the catalysts were characterized by XRD, H₂-TPR, CO₂-TPD, and SEM methods. The comparative catalytic effects of ZrO₂ and MgZrO_x catalysts were discussed under different reaction conditions. The reaction results showed that the addition of Mg to a ZrO₂ catalyst reduced the selectivity of CO₂ by inhibiting the water–gas conversion reaction, and increased the selectivity of aromatics and the proportion of BTX in aromatic products.

Keywords: syngas; direct synthesis; aromatics; Mg-modified ZrO₂ catalyst



Citation: Ma, D.; Sun, L.; Chen, L.; Yang, S.; Xie, X.; Si, H.; Zhao, B.; Hua, D. The Direct Synthesis of Aromatic Hydrocarbons from Syngas over Bifunctional MgZrO_x/HZSM-5 Catalysts. *Catalysts* **2023**, *13*, 997. <https://doi.org/10.3390/catal13060997>

Academic Editors: Benoît Louis and Anastasia Macario

Received: 21 March 2023

Revised: 30 April 2023

Accepted: 3 May 2023

Published: 13 June 2023



Copyright: © 2023 by the authors. Licensee MDPI, Basel, Switzerland. This article is an open access article distributed under the terms and conditions of the Creative Commons Attribution (CC BY) license (<https://creativecommons.org/licenses/by/4.0/>).

1. Introduction

Aromatic hydrocarbons are important basic chemical raw materials which are widely used in plastics, nylon, spices, and in other chemical synthesis processes. Aromatic hydrocarbons are currently being produced from the reforming and cracking of petroleum, which has caused environmental pollution and has also aggravated the consumption of fossil energy.

However, the syngas obtained from coal, natural gas, and biomass can be directly transformed into aromatics through catalysis processes, which are a new non-petroleum aromatics production route [1–3]. The syngas were firstly converted into methanol, dimethyl ether, or ketene and other oxygen-containing intermediates over the metal oxide catalyst in one step, and then olefins were produced through C-C coupling reactions over the zeolite molecular sieves or other solid acids, which were further transformed into aromatics through oligomerization, cyclization, and isomerization reactions. The direct synthesis of aromatics from syngas can effectively reduce the cost and energy consumption of the process and enhance the market competitiveness of aromatic products [4,5].

ZrO₂ oxide catalysts were widely used as the active metals in the direct production of aromatics from syngas, which have strong CO activation ability and high aromatic selectivity. When the ZrO₂ catalyst was used in the direct synthesis of aromatics from syngas, due to ZrO₂ being a non-redox metal, CO was not dissociated and adsorbed on its surface but could consume extra H₂ to reduce the O atoms in CO and then increase the conversion of CO [6]. However, the hydrogen dissociation ability of ZrO₂ catalysts is weak, and the CO conversion rate is low when catalyzing the syngas to oxygen-containing intermediates. Zn, Ce, Cu, and other hydrogen dissociation additives were added to modify ZrO₂ catalysts. An appropriate amount of metal oxide doping can promote the formation of oxygen defects and the activation of CO, resulting in an improvement in catalytic performance and the diversification of aromatics to benzene, toluene, xylene (BTX), as the representative of light aromatics, and tetramethyl benzene [3,7,8].

In the study of Cheng et al. [9], Zn-Zr-doped metal oxide catalysts were prepared and coupled with an HZSM-5 molecular sieve as a bifunction catalyst. Under the condition

of 450 °C, 3 MPa, and a hydrogen–carbon ratio (H_2/CO) = 2, the CO conversion rate was 9.6%, and the selectivity of CO_2 was 36%, while the selectivity of aromatics was 46%. Zhou et al. [10] prepared the Ce-Zr oxide catalysts and applied them to the transformation of syngas to produce aromatics. Under the conditions of 400 °C, 3 MPa, and H_2/CO = 2, the CO conversion rate was 1.2% and the aromatic selectivity was 75% under the action of $CeZrO_4/HZSM-5$ catalysts. The $CuZnAl-ZrO_2/Nb-ZSM-5$ catalysts were prepared and used in the syngas to aromatics reactions. It was found that with the increase in Zr content, the dispersion of Cu species was improved, and the conversion of CO and the selectivity of aromatics were also increased [11].

Although many studies have been conducted on the modification of Zr-based catalysts, there are still problems such as low aromatic selectivity, high selectivity of by-products CH_4 and CO_2 , poor catalyst stability, and so on [4,12]. In particular, the generation of CO_2 , the main by-product of aromatic hydrocarbons produced from syngas, was inhibited by adding CO_2 components to syngas raw materials. It has been reported that Mg oxides have strong reducibility and could strengthen the C-C coupling reaction and promote the chain growth of low carbon hydrocarbons. In addition, Mg oxides could also directly react with CO_2 to reduce the selectivity of CO_2 . However, it has not been reported that Mg-modified ZrO_2 catalysts were used in the direct synthesis of aromatics from syngas [13].

Therefore, in this paper, the Mg-modified ZrO_2 catalysts were first prepared and coupled with HZSM-5 zeolite catalysts through a mechanical mixing method, and were applied in the direct synthesis of aromatics from syngas. The catalysts were characterized by various methods, such as XRD, H_2 -TPR, CO_2 -TPD, and SEM. The effects of reaction conditions, such as temperature, pressure, and the mass ratio of metal oxides to molecular sieve, on the conversion of CO, and the selectivity of CO_2 and aromatics were carefully investigated.

2. Results and Discussion

2.1. Catalyst Characterization

2.1.1. XRD

The XRD patterns of the fresh ZrO_2 , $MgZrO_x$, $ZrO_2/HZSM-5$, and $MgZrO_x/HZSM-5$ catalysts are presented in Figure 1. The XRD diffraction peaks of the ZrO_2 catalyst after roasting are mainly tetragonal phase ($t-ZrO_2$), accompanied by a small amount of monoclinic phase ($m-ZrO_2$) peaks. The XRD diffraction peaks of $MgZrO_x$ catalysts were mainly $t-ZrO_2$, while the $m-ZrO_2$ peak disappeared and transformed into $t-ZrO_2$ with the doping of the Mg element, and no MgO phase was observed. Similar to the report of Huang et al., there is only a ZrO_2 peak in the XRD spectrum after the doping of the Zn metal element in a Zr-based catalyst. It is concluded that the solid solution structure is composed of the Mg element and the ZrO_2 metal oxide [14,15]. After the bifunctional catalyst was formed using a coupling molecular sieve, the XRD spectrum of $ZrO_2/HZSM-5$ and $MgZrO_x/HZSM-5$ retained the diffraction peak of the metal oxide catalyst, but only the diffraction peak of the molecular sieve was added, indicating that the mixing of the metal oxide catalyst and molecular sieve powder had no effect on the crystal phase of the catalyst.

Figure 2 shows the XRD patterns of ZrO_2 , $MgZrO_x$, $ZrO_2/HZSM-5$, and $MgZrO_x/HZSM-5$ catalysts after the reaction. Compared to Figure 1, it is found that the XRD diffraction peaks of the catalysts after the reaction are slightly reduced, which is believed to be caused by the covering of carbon generated in the reaction, and the accumulation and growth of catalyst particles after the reaction. However, the XRD diffraction peaks of the bifunction catalyst showed no additional diffraction peaks except for the peaks of HZSM-5 in the range from 10° to 25°, indicating that there was no additional phase after the metal oxide and HZSM-5 were physically mixed to form the bifunction catalyst. Additionally, the peak intensity of the bifunction catalyst decreased compared with the single metal oxide, which was believed to be caused by the reduction of the metal oxide [8,16].

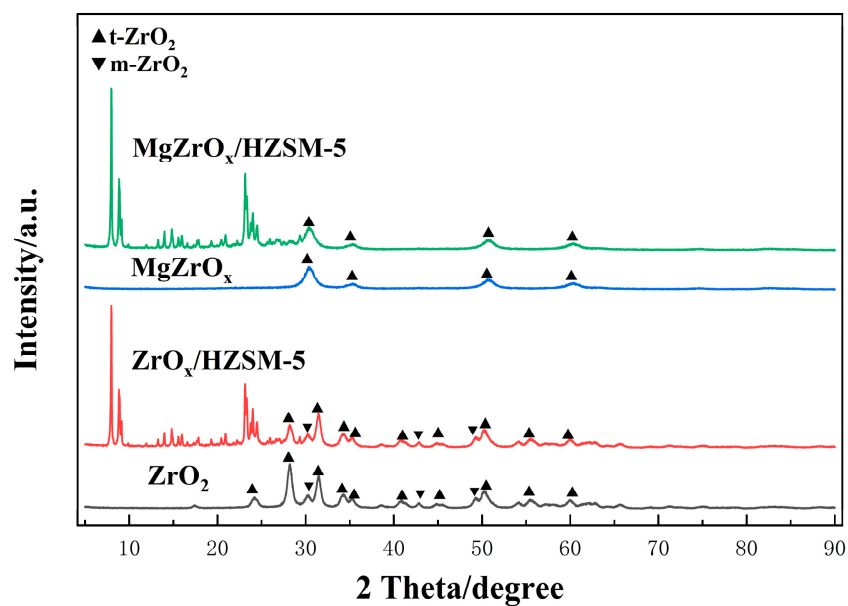


Figure 1. XRD pattern of the fresh catalysts.

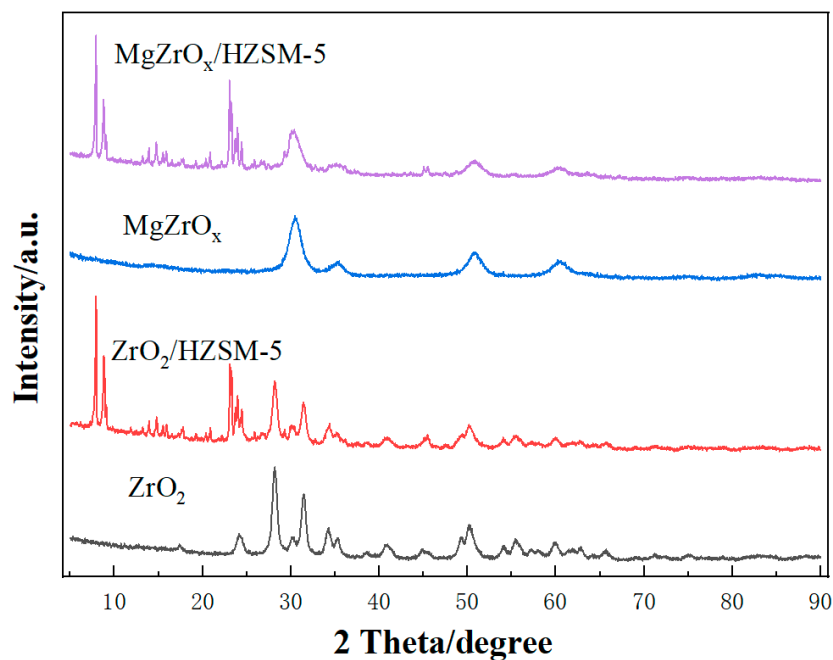


Figure 2. XRD pattern of the used catalysts.

Figure 3 shows the XRD patterns of the used $\text{MgZrO}_x/\text{HZSM-5}$ catalysts which reacted at different temperatures and pressures. According to Figure 3, the XRD diffraction peaks of the used catalysts are basically the same, indicating that the crystal phase and structure of the bifunction catalysts are stable. After the complex experimental conditions and long-term reaction, the original crystal phase remains unchanged and the catalyst structure remains intact without defects such as collapse [17].

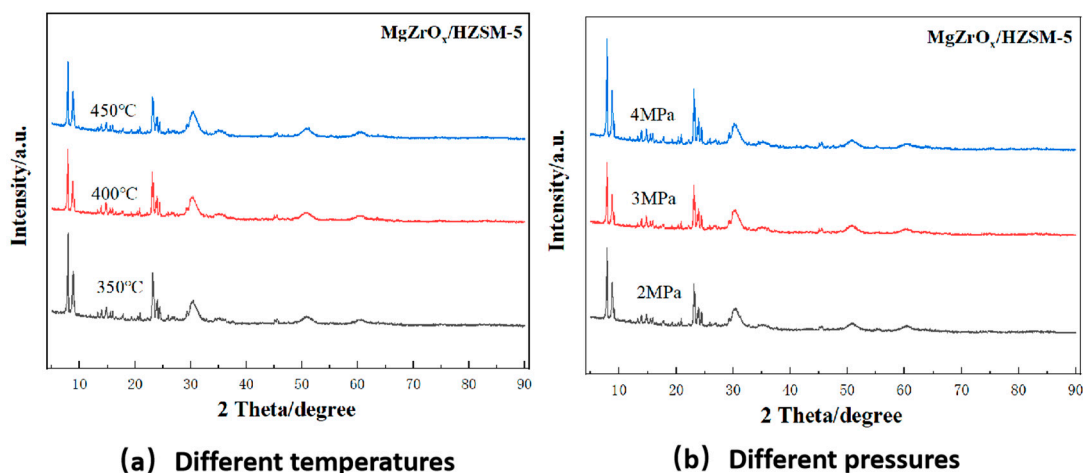


Figure 3. XRD patterns of the used MgZrO_x/HZSM-5 catalysts under different experimental conditions. (a) Different temperatures. (b) Different pressures.

2.1.2. SEM

The SEM images of the fresh catalysts are shown in Figure 4. According to Figure 4a,b, the fresh metal oxide catalyst shows that small particles are mixed with each other and are agglomerated. In Figure 4c,d, after the fresh metal oxide catalyst and HZSM-5 were coupled to form a dual-functional catalyst by mechanical mixing, it was observed that some metal nanoparticles gathered on the HZSM-5 in an irregular form, while some metal nanoparticles and molecular sieves gathered separately. According to Figure 4e, it is observed that the morphology of fresh HZSM-5 is hexagonal square [18,19].

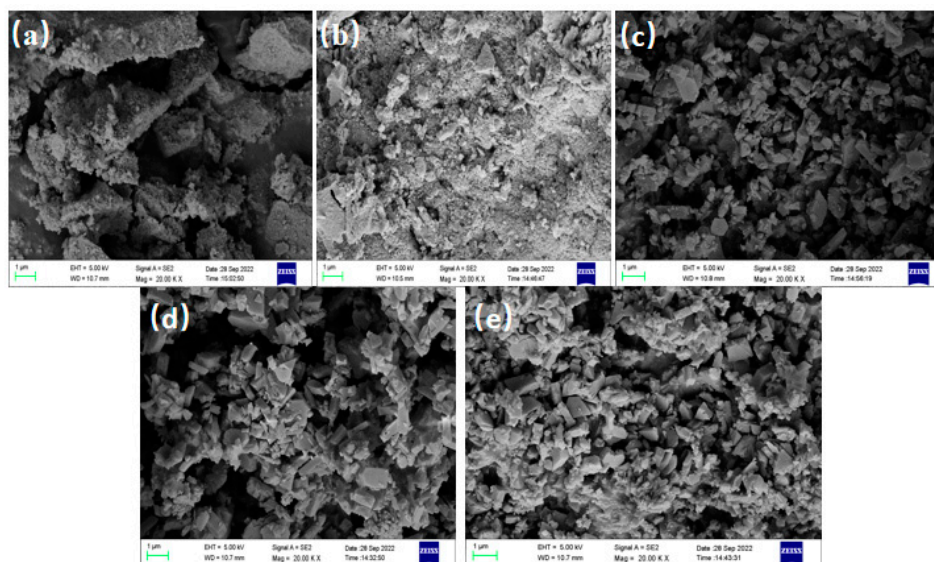


Figure 4. SEM images of the fresh catalysts. (a) ZrO₂. (b) MgZrO_x. (c) ZrO₂/HZSM-5. (d) MgZrO_x/HZSM-5. (e) HZSM-5.

Figure 5 shows the SEM images of the used catalysts. According to Figure 5a,b, after the CO hydrogenation reaction, the metal nanoparticles sintered and aggregated into large nanoparticles and clusters, and the surface of the catalysts showed flocculent carbon deposition [20]. The morphology of the HZSM-5 remained basically unchanged, and it was observed that the metal nanoparticles did not flow and redistribute on the HZSM-5 through Figure 5c,d, indicating that the migration of ZrO₂ and MgZrO_x species combined with HZSM-5 would not lead to the deactivation of the catalyst [21].

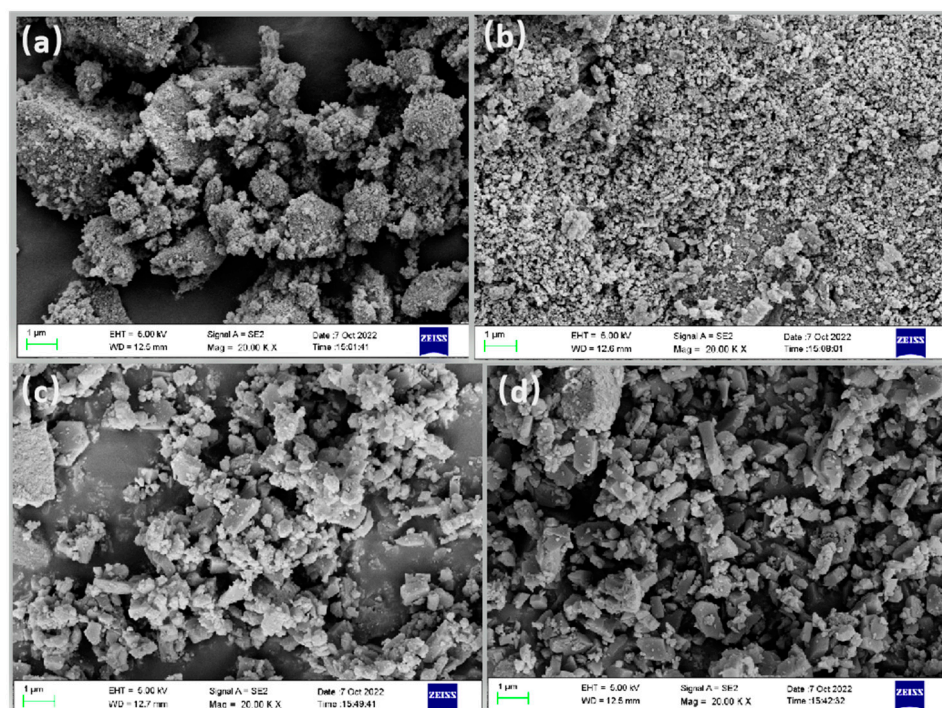


Figure 5. SEM images of the used catalysts. (a) ZrO_2 . (b) MgZrO_x . (c) $\text{ZrO}_2/\text{HZSM-5}$. (d) $\text{MgZrO}_x/\text{HZSM-5}$.

2.1.3. H_2 -TPR

The H_2 -TPR diagrams of the fresh catalysts are shown in Figure 6. According to Figure 6, there is no reduction peak in the H_2 -TPR profiles of the fresh ZrO_2 catalyst, which is because the reduction temperature of ZrO_2 is higher than $700\text{ }^\circ\text{C}$, indicating that there is no valence change in the metal oxide in the range of $100\text{--}800\text{ }^\circ\text{C}$. For the MgZrO_x catalyst, there is a small reduction peak near the high temperature of $500\text{ }^\circ\text{C}$, which is considered to be a partial reduction of the MgZrO_x solid solution structure. The common reaction temperature of the syngas through methanol to aromatics is $300\text{--}500\text{ }^\circ\text{C}$, so the selected catalysts can stably exist under the common reaction conditions of the direct synthesis of aromatics from syngas, which can improve the catalytic performance of the catalysts [22].

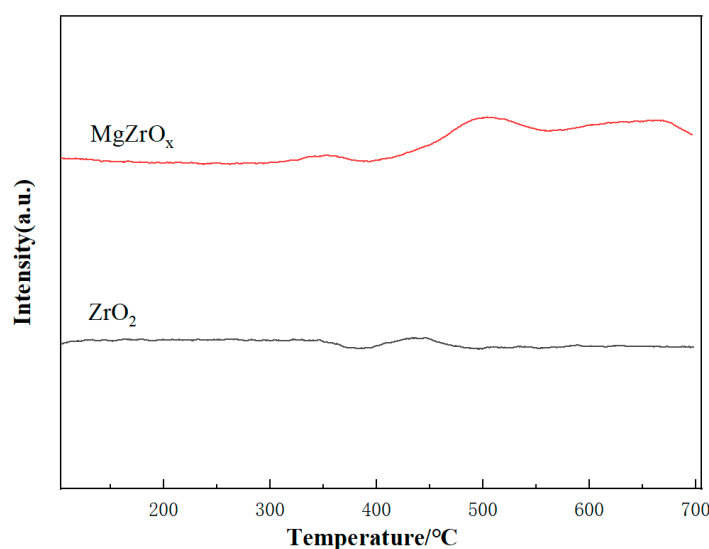


Figure 6. H_2 -TPR diagrams of the fresh catalysts.

2.1.4. CO₂-TPD

The basicity of ZrO₂ and MgZrO_x catalysts was detected by CO₂-TPD, and the profiles are shown in Figure 7. There is only one single large desorption peak for the ZrO₂ and MgZrO_x catalysts, and the ZrO₂ metal oxide is near 90 °C, while the MgZrO_x-doped metal oxide is near 120 °C. After the doping of the Mg element, the CO₂ desorption peak migrated towards high temperature and the peak area increased, indicating that the MgZrO_x catalyst had a stronger physical adsorption capacity and alkalinity for CO₂ than the ZrO₂ catalyst [15,23,24].

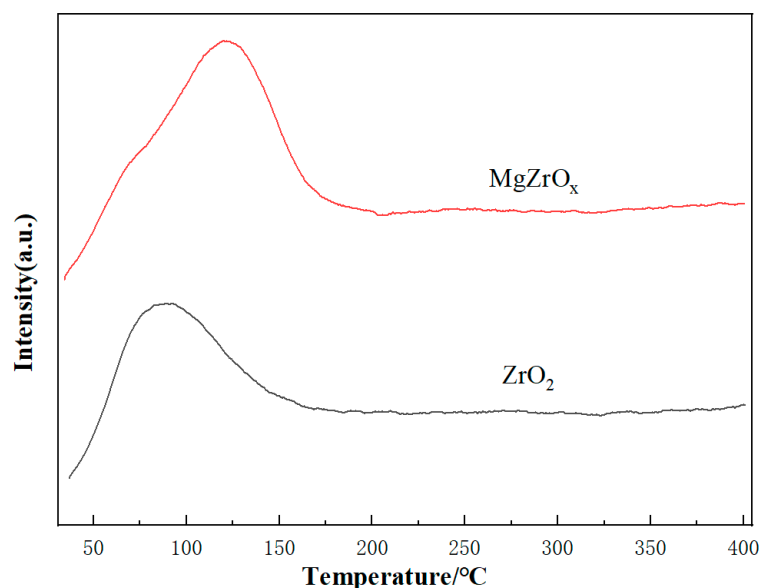


Figure 7. CO₂-TPD of the fresh catalysts.

2.2. Catalyst Performance

2.2.1. Effect of Mg Doping on the Performance of Zr-Based Catalysts for Direct Syngas Conversion to Aromatics

The reaction performances of direct syngas conversions to aromatics on different Zr-based catalysts and HZSM-5 mixed bifunctional catalysts are presented in Figure 8. The CO conversion of the ZrO₂ catalyst is 14.4% and the selectivity of C₅₊ and oxygenates is 67.5%. After doping Mg, the conversion of CO for the MgZrO_x catalyst decreases to 12.7%, and the selectivity of the CO₂ decreases (18.5–10.3%), while the selectivity of C₅₊ and oxygenates increases to 75.4%. Compared with the ZrO₂/HZSM-5 catalyst, the conversion of CO for MgZrO_x/HZSM-5 decreased from 20.2% to 15.8% after coupling with HZSM-5, and the selectivity of CO₂ decreased slightly (21–17%), while the selectivity of C₅₊ and oxygenates products increased (63–67%). The results showed that the addition of the molecular sieve did not change the influence of the Mg-modified Zr-based catalyst on the catalytic performance of the synthesis of gas to aromatics, which was manifested by the reduction in CO conversion, the reduction in CO₂ selectivity, and the increase in C₅₊ product selectivity. The reduction in CO₂ selectivity is caused by the fact that metal Mg can reduce the activity of the water–gas shift reaction and it can increase the activity of the C–C coupling reaction, promoting the generation of low-carbon olefins and thus increasing the selectivity of C₅₊ products [25]. Similar to the Ce element doped in the ZrO₂ catalyst reported by Zhou et al. [10], the conversion of CO did not increase, indicating that neither the doping of Ce nor Mg could promote the adsorption and conversion of CO.

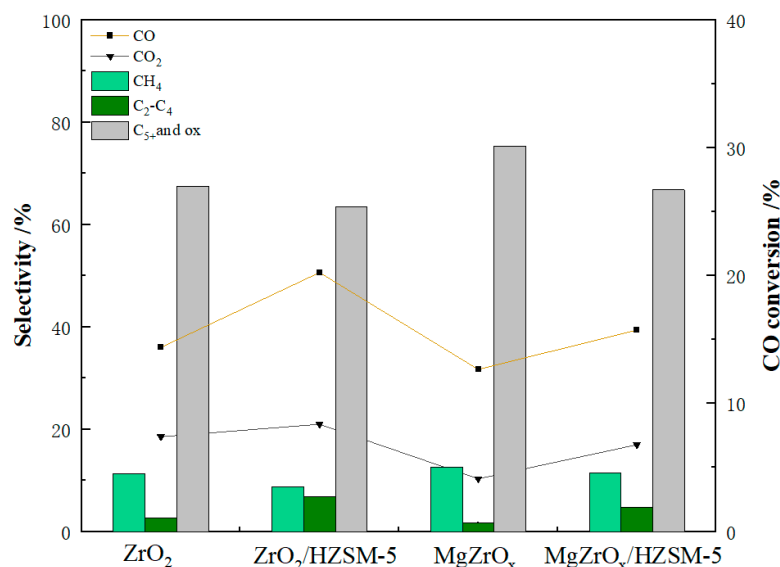


Figure 8. Catalytic performance of different Zr-based metal oxides and HZSM-5 mixed bifunctional catalyst in direct syngas conversion to aromatics. C₂–C₄: including paraffins and olefins. C₅₊ and ox: C₅₊ hydrocarbons and oxygenates. Reaction conditions: 400 °C, 3 MPa, syngas (H₂/CO = 2) with flow rate of 20 mL/min, metal oxide catalyst 0.5 g, bifunction catalyst 1 g, time on stream of 20 h.

Figure 9 shows the distribution of C₅₊ hydrocarbons and oxygenates on individual metal oxide catalysts. According to Figure 9, the majority of the liquid phase products of ZrO₂ single metal oxide catalysts are methanol (94%) and some long-chain hydrocarbons, and so the intermediate product is believed to be methanol, which is consistent with the results reported by previous studies [17]. The liquid phase product of MgZrO_x catalyst contains not only methanol (27%) but also includes a large amount of propanol (61%) and some relatively long-chain hydrocarbons. It is considered that the low CO conversion of the MgZrO_x catalyst is due to its weak ability to produce methanol and because the reaction intermediate contains propanol.

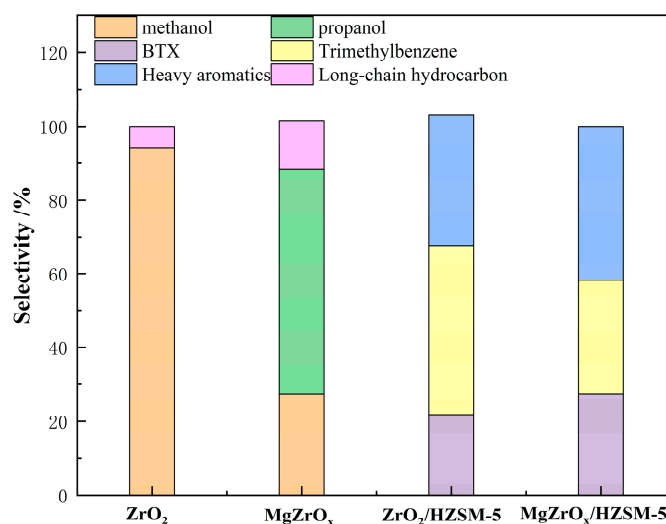


Figure 9. The distribution of C₅₊ hydrocarbons and oxygenates on different Zr-based metal oxides and HZSM-5 mixed bifunctional catalyst. BTX: benzene, toluene, and xylene. Heavy aromatics: C₉₊ aromatics.

The distributions of C₅₊ hydrocarbons and oxygenates on different bifunctional catalysts and the MgZrO_x/HZSM-5 catalysts are shown in Figure 9. Compared to the ZrO₂/HZSM-5 catalyst, the BTX component in the liquid products of the MgZrO_x/HZSM-5

catalyst increases to 27.4%, and the content of trimethylbenzene decreases to 30.7%, while the content of heavy aromatics increases. Furthermore, no long-chain hydrocarbon appears in the liquid products of $\text{ZrO}_2/\text{HZSM-5}$ and $\text{MgZrO}_x/\text{HZSM-5}$ catalysts. The above results indicate that the doping of Mg is conducive to the formation of BTX and heavy aromatics. Compared to the molecular sieves modified by Mg, reported by Yang et al. [23], at the cost of reducing the selectivity of aromatics and increasing the selectivity of xylene, doping Mg into metal oxide catalysts can not only increase the proportion of BTX in liquid phase products, but can also increase the selectivity of aromatic products.

2.2.2. Effects of Temperatures

Generally, the CO conversion rate of the bifunctional catalyst increases with the increase in temperature. In order to study the effect of reaction temperature on the direct synthesis of aromatic hydrocarbons from syngas using a $\text{MgZrO}_x/\text{HZSM-5}$ catalyst, the reaction temperature ranged from 350 °C to 450 °C, while the other reaction conditions were fixed. The effects of reaction temperatures on the catalytic performance of $\text{MgZrO}_x/\text{HZSM-5}$ are shown in Figure 10. The conversion rate of CO linearly increases to 20.4% with the increase in temperature, and the selectivity of CO_2 does not change obviously at a low temperature, being about 17%. This is because as the reaction temperature increases, the reaction rate of the direct production of aromatic hydrocarbons from synthetic gas through oxygen-containing compounds increases, and the CO conversion rate also increases. However, when the temperature rises to 450 °C, the CO_2 selectivity increases to 21.4% due to the high temperature accelerating the water–gas shift reaction. The selectivity of methane first decreases with the increase in temperature, and then increases to 16% at a low temperature of 350 °C. The selectivity of C_{5+} products firstly increases and then decreases with increasing temperature, and reaches the maximum of 66.8% at 400 °C. In addition [26], it has been reported that the excessively high reaction temperature also easily leads to the hydrocracking of intermediates, so the selectivity of low carbon hydrocarbon products increases to 11.5% at a high temperature of 450 °C. This is because although the water–gas shift reaction is thermodynamically advantageous at a low temperature, it is subjected to the kinetic limitation of the C–C coupling reaction catalyzed by molecular sieves. When the temperature is too high, the water–gas shift reaction is also likely to occur, but the reaction activity of intermediate hydrocracking is too high; therefore, a large number of low-carbon hydrocarbon products are generated, and then the aromatization reaction is inhibited [27]. Similar to the study of the $\text{Zn-ZrO}_2/\text{HZSM-5}$ catalyst by Wang et al. [16], with the increase in reaction temperature from 320 °C to 400 °C, the conversion of CO increased from 22.1% to 48.4%, the selectivity of aromatics increased at first and then decreased, and the highest selectivity was 73.1% at 360 °C.

According to Figures 10 and 11, the reaction temperatures have a significant influence on the distribution of liquid products. When the temperature is 350 °C, the BTX component of light aromatic hydrocarbons is only 18.7%, and the heavy aromatics and trimethylbenzene account for 38.4% and 35.7%, respectively, while the liquid products contain a small number of long-chain hydrocarbon products (7.2%) due to the decrease in catalyst activity at a low temperature [28]. With the increase in temperature, the reaction activity and rate of synthesis of gas to aromatics increase, and the production of aromatics is improved, but when the temperature is too high, it will promote the hydrocracking of intermediates and the hydro isomerization of aromatics, and reduce the selectivity of light aromatic products [29]. When the temperature rises to 450 °C, the proportion of long-chain hydrocarbons in liquid products is relatively high (12.61%), and the proportion of the BTX component of light aromatics is 22%, and due to that the hydrocracking reaction is severe. For the temperature of 400 °C, the total C_{5+} selectivity of the products was the highest and the BTX component reached the maximum of 27.4% in the liquid phase products because the aromatization ability was strong and no long-chain hydrocarbon products were generated at the temperature of 400 °C. Similar to the study of the $\text{Cr}_2\text{O}_3/\text{ZSM5}$ catalyst by Liu et al. [30], with the increase in reaction temperature from 375 °C to 415 °C,

the proportion of BTX in the liquid phase products increased at first and then decreased, and the highest proportion was 47.3% at 395 °C.

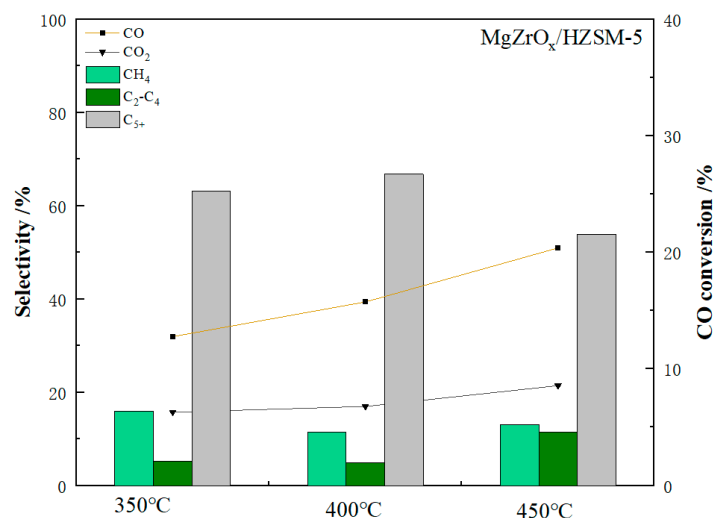


Figure 10. The effect of temperature on CO conversion and product selectivity of MgZrO_x/HZSM-5 catalysts. Reaction conditions: 3 MPa, syngas (H₂/CO = 2) with flow rate of 20 mL/min, metal oxide catalyst 0.5 g, bifunction catalyst 1 g, time on stream of 20 h.

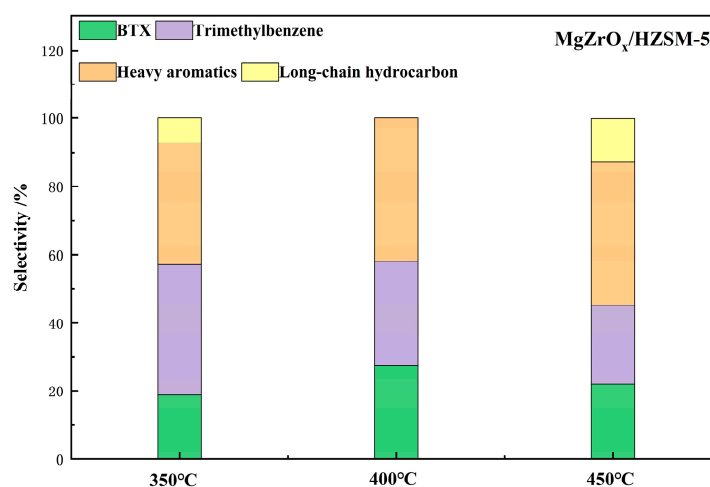


Figure 11. The distribution of C₅₊ hydrocarbons products in MgZrO_x/HZSM-5 catalysts at different temperatures.

2.2.3. Effect of Pressures

In order to study the effect of reaction pressure on the direct synthesis of aromatic hydrocarbons from syngas on a MgZrO_x/HZSM-5 catalyst, the reaction pressure ranged from 2 MPa to 4 MPa, while the other reaction conditions were fixed. Figure 12 shows the effect of pressure on the catalytic performance of MgZrO_x/HZSM-5. As the reaction pressure increases from 2 MPa to 4 MPa, the CO conversion rate increases from 13.3% to 19.2%. This is due to the fact that the volume of the reaction of syngas to aromatics from oxygen-containing intermediates decreases, so increasing the reaction pressure can significantly increase the CO conversion but has little effect on aromatic selectivity [31]. When the pressure is low (less than 3 MPa), the selectivity of C₅₊ and CO₂ products does not obviously change, being about 66.8% and 17%, respectively. However, when the pressure rose to 4 MPa, the selectivity of methane increased to 17.8%, the selectivity of low carbon hydrocarbons increased to 8.26%, and the selectivity of C₅₊ products decreased to 51%

because high pressure results in an increase in hydrogenation activity [26]. Similar to the effect of pressure on $\text{ZnCr}_2\text{O}_4/\text{ZSM-5}$ catalysts reported by Yang et al. [27], the increasing pressure in the range of 1 MPa–3 MPa can significantly increase the conversion of CO, while the selectivity of aromatic products shows little change.

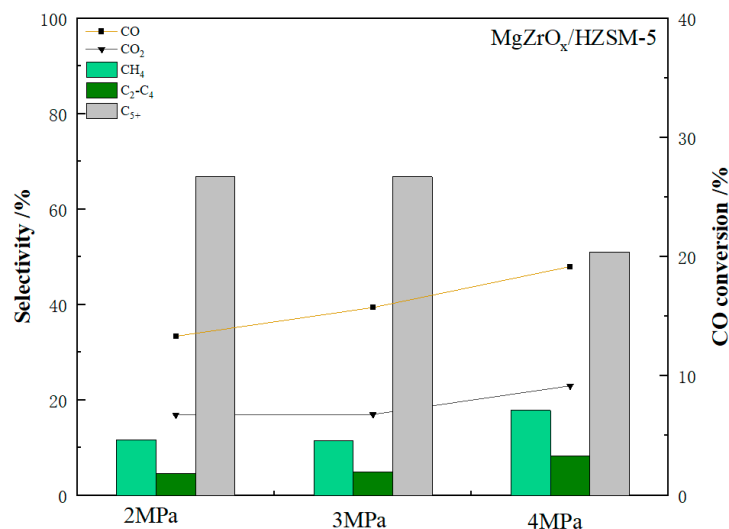


Figure 12. The effect of pressures on CO conversion and product selectivity of $\text{MgZrO}_x/\text{HZSM-5}$ catalysts. Reaction conditions: 400 °C, syngas ($\text{H}_2/\text{CO} = 2$) with flow rate of 20 mL/min, metal oxide catalyst 0.5 g, bifunction catalyst 1 g, time on stream of 20 h.

Figure 13 shows a schematic diagram of the distribution of liquid products on the $\text{MgZrO}_x/\text{HZSM-5}$ catalyst with pressure change. With the increase in pressure from 2 MPa to 4 MPa, most of the liquid products are aromatics, and the proportion of heavy aromatics increases (35.3–48.1%), while the proportion of trimethyl benzene decreases (33.7–26.4%). This result is due to the higher activity of the carbon chain growth reaction under high pressure, resulting in an increase in selectivity for heavy aromatic hydrocarbons [32]. The proportion of the BTX component was not obviously changed at a low pressure (less than 3 MPa), being about 27.8%. When the pressure is 2 MPa, the liquid products contain a small number of long-chain hydrocarbon products (7.2%) because the low pressure weakens the aromatization ability. When the pressure rises to 4 MPa, the BTX component of light aromatic hydrocarbons is 24.5%, and there are traces of long-chain hydrocarbons (0.96%) because of the carbon chain growth of the intermediate and the strong isomerization activity of aromatics. Similar to the study of $\text{Cr}_2\text{O}_3/\text{ZSM-5}$ catalysts by Liu et al. [30], there is little change in the proportion of BTX components with the increase in pressure.

2.2.4. Effect of Mass Ratio of Metal Oxide to HZSM-5

Generally, when the mass ratio of metal oxide to HZSM-5 increases, the CO conversion rate increases, and more intermediates are generated to promote the production of aromatics. However, when it is too high, the selectivity of low carbon hydrocarbons will increase due to the excessive hydrogenation of products. With the decrease in the mass ratio of metal oxide to HZSM-5, the aromatization ability is enhanced, and the conversion of syngas is also driven by promoting the consumption of intermediates [33]. In order to study the effect of mass ratio of metal oxide to HZSM-5 on the direct synthesis of aromatic hydrocarbons from syngas on a $\text{MgZrO}_x/\text{HZSM-5}$ catalyst, the mass ratio of metal oxide to HZSM-5 ranged from 2:1 to 1:3 while the other reaction conditions were fixed.

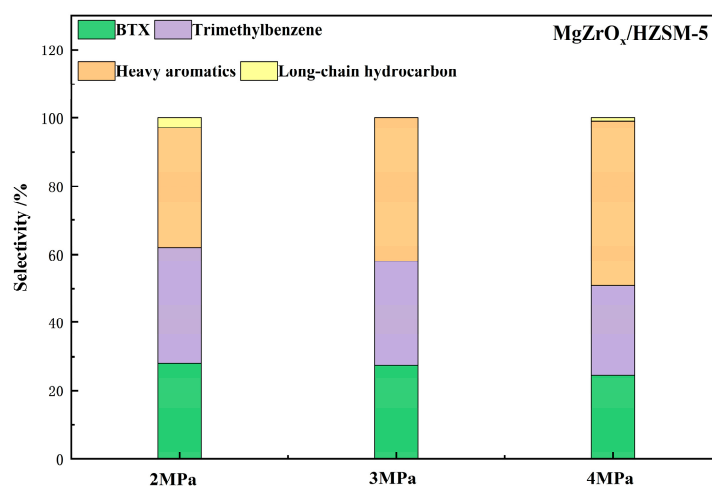


Figure 13. The distribution of C₅₊ hydrocarbons products in MgZrO_x/HZSM-5 catalysts at different pressures.

Figure 14 shows the variation in CO conversion and product selectivity catalyzed by MgZrO_x/HZSM-5 at different mass ratios. As the increase in the mass ratio of metal oxides to HZSM-5 increases from 1:3 to 2:1, the CO conversion rate slowly increases from 13.1% to 16%. The results showed that when the mass ratio of metal oxide catalysts increased, the conversion of CO slightly increased, which corresponds to the decrease in CO conversion after doping Mg in the initial experiment [34]. When the mass ratio of MgZrO_x to HZSM-5 is too low (1:3) or too high (2:1), the doping of Mg cannot reduce the generation of CO₂, the selectivity of which is about 20% [8]. With the increase in the mass ratio of metal oxides to HZSM-5, the selectivity of low carbon hydrocarbons decreases (6.5–4.1%) as the ability of the bifunctional catalyst to convert syngas increases. In the larger mass ratio range (2:1–1:2), the selectivity of C₅₊ products does not obviously change, being about 65%. When the mass ratio of metal oxides to HZSM-5 was too low (1:3), the selectivity of C₅₊ products decreased to 58.7%, and the selectivity of methane increased to 15.6% because the MgZrO_x catalyst could not provide enough intermediate products during the reaction. Compared with the study of Cheng et al. [27], the mass ratio of metal oxides to molecular sieves to Zn-ZrO₂/ZSM-5 catalysts decreased from 2:1 to 1:2, and the aromatic selectivity increased from 61% to 73%, but the CO conversion of the catalyst decreased significantly from 32% to 16%. It is considered that the different changes in CO conversion are due to the inability of Mg doping to promote CO adsorption activation.

Figure 15 shows the variation in the liquid phase product distribution of MgZrO_x/HZSM-5 catalyst under the different mass ratios of metal oxide to HZSM-5. When the mass ratio of metal oxides to HZSM-5 is 1:3–1:1, the liquid products are almost equal to the aromatic products. However, when the mass ratio of metal oxides to HZSM-5 rises to 2:1, the liquid products contain a large number of long-chain hydrocarbons (23.35%) and the BTX component is smaller, about 25%, as the high content of metal oxide means the HZSM-5 cannot rapidly convert the intermediates. When the mass ratio of metal oxide to HZSM-5 is 1:3, the BTX component in the liquid product reaches the maximum of 35.3%, but the overall content of the BTX component is not high, and, due to that, the C₅₊ selectivity is low under this condition (58.7%). When the mass ratio of HZSM-5 to the metal oxide catalyst was 2:1, the selectivity of the C₅₊ product was 65%, and the BTX component of the liquid phase product was 32.2%. This indicates that sufficient amounts of the HZSM-5 molecular sieve are required by the dual-function catalyst for the conversion of oxygen-containing intermediates to aromatics through the oligomerization, cyclization, and isomerization reactions [17]. Similarly, Cheng et al. reported that when the mass ratio of metal oxide catalyst to molecular sieve decreased from 2:1 to 1:2, the selectivity of long-chain hydrocarbons in liquid products decreased from 7.4% to 2%, and the selectivity of target product aromatics increased to 73% for the ZnO-ZrO₂/HZSM-5 catalyst [9].

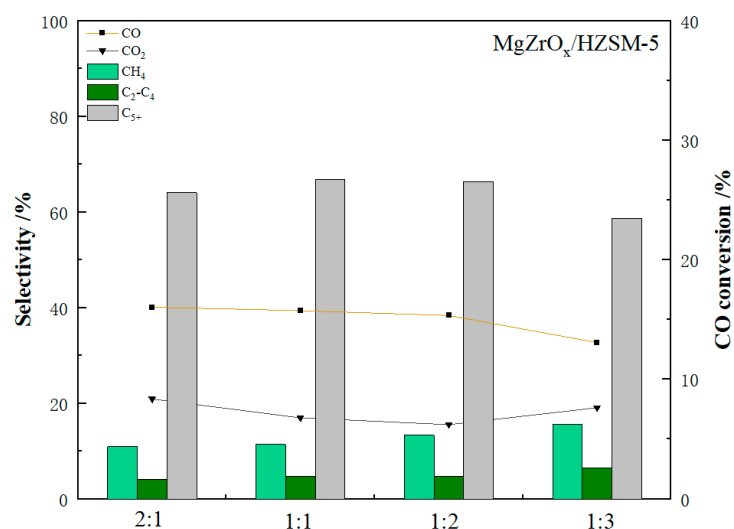


Figure 14. The effect of mass ratio of metal oxide catalyst to HZSM-5 on CO conversion and product selectivity of MgZrO_x/HZSM-5 catalysts. Reaction conditions: 400 °C, 3 MPa, syngas (H₂/CO = 2) with flow rate of 20 mL/min, bifunction catalyst 1 g, time on stream of 20 h.

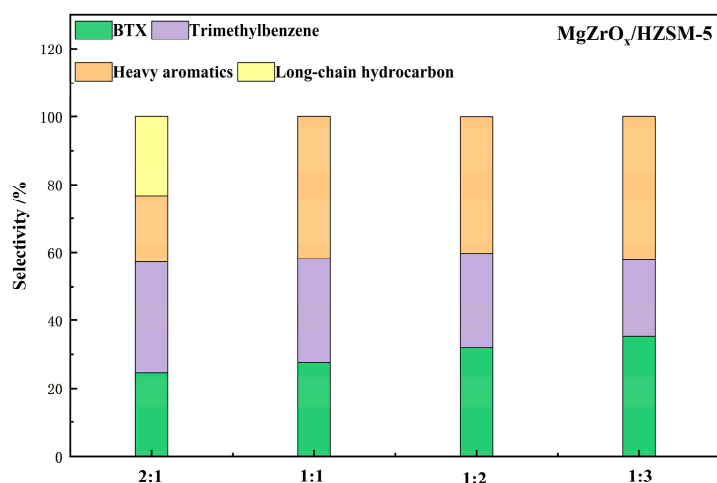


Figure 15. The distribution of C₅₊ hydrocarbons products in MgZrO_x/HZSM-5 catalysts at different mass ratios of metal oxide catalyst to HZSM-5.

3. Materials and Methods

3.1. Catalyst Preparation

ZrO₂ and MgZrO_x catalysts were prepared by a co-precipitation method. Firstly, stoichiometric quantities of zirconium nitrate and magnesium nitrate were added into 100 mL of water to make a solution. Secondly, a certain proportion of ammonia solution was added into the mixed aqueous solution at 85 °C with constant stirring; the pH was controlled to 10 in order to fully precipitate the metal salts. The precipitate was collected by filtration and thoroughly washed with distilled water. Then, the solid products were dried overnight at 110 °C and calcined in air at 500 °C for 4 h to obtain MgZrO_x catalysts [4]. HZSM-5-117 zeolite catalysts were purchased from Tianjin Nankai Catalyst Industry. After grinding and mixing with ZrO₂ or MgZrO_x catalysts in an agate mortar, the bifunction catalysts were obtained.

3.2. Catalyst Characterization

The H₂ temperature programmed reduction (H₂-TPR) was carried out on the FINESORB-3010 instrument. First, 0.05 g catalyst samples were heated at room temperature to 800 °C in an Ar atmosphere for pretreatment. After being cooled to 100 °C, the catalysts

were heated with a 10% H₂/Ar mixture from 100 °C to 900 °C at a rate of 10 °C/min. The signals were detected by the thermal conductivity detector (TCD).

XRD analysis was carried out using a PANalytical Empyrean X-ray diffractometer with a Cu K α ray, tube voltage of 40 kV, tube current of 40 mA, and a scanning angle from 5° to 90°.

The micromorphology and microstructure of the catalyst were observed with Zeiss SUPR-55 scanning electron microscopy (SEM), and with accelerated voltage of 0.1 to 30 kV. Before the test, small amounts of samples should be fixed on the conductive adhesive and treated with gold spray to enhance the conductivity of the sample.

The CO₂ temperature-programmed desorption experiments (CO₂-TPD) were also performed using the FINESORB-3010 instrument. The 0.05 g sample was weighed and placed in the reaction tube. The sample was heated at 10 °C/min from room temperature to 300 °C for drying pretreatment. The sample was purged by Ar stream for 1 h and cooled to 50 °C. The 10% CO₂/Ar mixture was injected for 1 h to saturation, and then Ar flow was switched to purge for 1 h to remove the weak physical adsorption CO₂ on the surface. Finally, the catalysts were increased to 800 °C at a rate of 10 °C/min in Ar, and the signal was detected by TCD.

3.3. Catalytic Reaction

The experiments involving the direct synthesis of aromatics from syngas were carried out in a fixed-bed reactor. The quartz tube, with an inner diameter of 7 mm and length of 400 mm, was kept in the electric heating furnace with a height of 500 mm and a width of 300 mm. The reaction temperature was measured by one K-type thermocouple placed in the inside tube with one end in the middle of the catalyst bed. During the experiment, a certain pressure of syngas is slowly introduced into the reactor, and the pressure and temperature are gradually adjusted to the reaction pressure and reaction temperature, respectively. The outflow products from the reactor were passed through the cold trap and the back pressure valve, respectively. The liquid products generated by the reaction were collected by the condensing device. The other small molecules' gases were collected by the air bag at a certain interval and were analyzed via the gas chromatograph. CO conversion and CO₂ selectivity (Sel_{CO₂}) and individual hydrocarbon C_nH_m selectivity (Sel_{C_nH_m}) are calculated as follows:

$$\text{Con}_{\text{CO}} = \frac{\text{CO}_{\text{in}} - \text{CO}_{\text{out}}}{\text{CO}_{\text{in}}} \times 100\% \quad (1)$$

where CO_{in} and CO_{out} represent moles of CO at the inlet and outlet.

$$\text{Sel}_{\text{CO}_2} = \frac{\text{CO}_{2\text{out}}}{\text{CO}_{\text{in}} - \text{CO}_{\text{out}}} \times 100\% \quad (2)$$

where CO₂ outlet denotes moles of CO₂ at the outlet.

$$\text{Sel}_{\text{C}_n\text{H}_m} = \frac{n\text{C}_n\text{H}_{m\text{out}}}{\sum_1^n n\text{C}_n\text{H}_{m\text{out}}} \times 100\% \quad (3)$$

where C_nH_m outlet denotes moles of C_nH_m at the outlet.

4. Conclusions

ZrO₂ and MgZrO_x catalysts were prepared by the co-precipitation method, and then combined with HZSM-5 to form the bifunctional catalyst, which was used in the direct synthesis of aromatic hydrocarbons from syngas. The characterization and experimental results show that at 400 °C, 3 MPa, H₂/CO = 2 and a mass ratio of metal oxide to HZSM-5 of 1:2, the MgZrO_x catalyst displayed the best activity with a CO conversion of 15.3%, CO₂ selectivity of 15.5%, and aromatic selectivity of 66.4%. Under the above reaction conditions, CO activation ability is high, and HZSM-5 can also efficiently transform methanol and other oxygen-containing intermediates into target aromatic products by avoiding the generation

of long-chain hydrocarbons and reducing the selectivity of heavy aromatics, thus improving the proportion of BTX components. In summary, with the doping of Mg on ZrO₂, the modified MgZrO_x catalysts could reduce the selectivity of CO₂ and improve the selectivity of aromatic products and the proportion of BTX components in liquid products during the direct synthesis of aromatic hydrocarbons from syngas.

Author Contributions: Conceptualization, D.M. and L.S.; formal analysis, L.C.; funding acquisition, L.S. and B.Z.; investigation, D.M., S.Y. and H.S.; methodology, H.S. and L.C.; project administration, D.M. and L.S.; resources, D.H. and X.X.; supervision, L.S.; validation, L.S.; writing—original draft, D.M.; writing—review and editing, L.S. All authors have read and agreed to the published version of the manuscript.

Funding: This work was supported by the National Natural Science Foundation of China (No.21908117), Natural Science Foundation of Shandong Province (No.ZR2022MB059, ZR2021QB156), Jinan City's "20 New Colleges and Universities" project (202228018), the Key Research and Development Program of Shandong Province (2022CXGC010701) and the Education and Industry integration innovation pilot Project (2022JBZ02-03).

Data Availability Statement: Not applicable.

Conflicts of Interest: The authors declare no conflict of interest.

References

- Colak, N.S.; Kalay, E.; Sahin, E. Asymmetric reduction of prochiral aromatic and hetero aromatic ketones using whole-cell of *Lactobacillus senmaizukei* biocatalyst. *Synth. Commun.* **2021**, *51*, 2305–2315. [[CrossRef](#)]
- Nikitas, N.F.; Apostolopoulou, M.K.; Skolia, E.; Tsoukaki, A.; Kokotos, C.G. Photochemical activation of aromatic aldehydes: Synthesis of amides, hydroxamic acids and esters. *Chem. A Eur. J.* **2021**, *27*, 7915–7922. [[CrossRef](#)] [[PubMed](#)]
- Wang, Y.; Xu, J.; Li, Z.; Guan, S.; Zeng, Y.; Zhao, G.; Sun, H.; Wen, F.; Subhan, F. Direct synthesis of Zn-incorporated nano-ZSM-5 zeolite by a dry gel conversion method for improving catalytic performance of methanol to aromatics reaction. *J. Porous Mater.* **2021**, *28*, 1609–1618. [[CrossRef](#)]
- Fu, Y.; Ni, Y.; Zhu, W.; Liu, Z. Enhancing syngas-to-aromatics performance of ZnO&H-ZSM-5 composite catalyst via Mn modulation. *J. Catal.* **2020**, *383*, 97–102.
- Fu, Y.; Ni, Y.; Chen, Z.; Zhu, W.; Liu, Z. Achieving high conversion of syngas to aromatics. *J. Energy Chem.* **2022**, *66*, 597–602. [[CrossRef](#)]
- Pan, X.; Jiao, F.; Miao, D.; Bao, X. Oxide-zeolite-based composite catalyst concept that enables syngas chemistry beyond Fischer-Tropsch synthesis. *Chem. Rev.* **2021**, *121*, 6588–6609. [[CrossRef](#)]
- Sheng, H.; Fang, Y.; Huang, Y.; Huang, Z.; Shen, W.; Xu, H. Highly Active Cu-CeZrO_x/ZSM-5@Si Catalyst for Direct Conversion of Syngas to Aromatics. *Ind. Eng. Chem. Res.* **2022**, *61*, 12405–12414. [[CrossRef](#)]
- Yang, S.; Li, M.; Nawaz, M.A.; Song, G.; Xiao, W.; Wang, Z.; Liu, D. High selectivity to aromatics by a Mg and Na Co-modified catalyst in direct conversion of syngas. *ACS Omega* **2020**, *5*, 11701–11709. [[CrossRef](#)]
- Cheng, K.; Zhou, W.; Kang, J.; He, S.; Shi, S.; Zhang, Q.; Pan, Y.; Wen, W.; Wang, Y. Bifunctional catalysts for one-step conversion of syngas into aromatics with excellent selectivity and stability. *Chem* **2017**, *3*, 334–347. [[CrossRef](#)]
- Zhou, W.; Shi, S.; Wang, Y.; Zhang, L.; Wang, Y.; Zhang, G.; Min, X.; Cheng, K.; Zhang, Q.; Kang, J.; et al. Selective conversion of syngas to aromatics over a Mo-ZrO₂/HZSM-5 bifunctional catalyst. *Chemcatchem* **2019**, *11*, 1681–1688. [[CrossRef](#)]
- Xiao, W.; Li, M.; Nawaz, M.A.; Xu, L.; Song, G.; Wang, Z.; Liu, D. Integrated catalyst of CuZnAl-Zr and Nb-HZSM-5 for one-step synthesis of aromatics from syngas. *Chin. J. Chem.* **2020**, *38*, 1311–1316. [[CrossRef](#)]
- Wang, S.; Fang, Y.; Huang, Z.; Xu, H.; Shen, W. The effects of the crystalline phase of zirconia on C-O activation and C-C coupling in converting syngas into aromatics. *Catalysts* **2020**, *10*, 11. [[CrossRef](#)]
- Chen, H.; Lin, L.; Li, Y.; Wang, R.; Gong, Z.; Cui, Y.; Li, Y.; Liu, Y.; Zhao, X.; Huang, W.; et al. CO and H₂ Activation over g-ZnO Layers and w-ZnO(0001). *ACS Catal.* **2019**, *9*, 1373–1382. [[CrossRef](#)]
- Huang, Z.; Wang, S.; Qin, F.; Huang, L.; Yue, Y.; Hua, W.; Qiao, M.; He, H.; Shen, W.; Xu, H. Ceria-zirconia/zeolite bifunctional catalyst for highly selective conversion of syngas into aromatics. *Chemcatchem* **2018**, *10*, 4519–4524. [[CrossRef](#)]
- Tian, H.; He, H.; Jiao, J.; Zha, F.; Guo, X.; Tang, X.; Chang, Y. Tandem catalysts composed of different morphology HZSM-5 and metal oxides for CO₂ hydrogenation to aromatics. *Fuel* **2022**, *314*, 13. [[CrossRef](#)]
- Wang, Y.; Zhan, W.; Chen, Z.; Chen, J.; Li, X.; Li, Y. Advanced 3D hollow-out ZnZrO@C combined with hierarchical zeolite for highly active and selective CO hydrogenation to aromatics. *ACS Catal.* **2020**, *10*, 7177–7187. [[CrossRef](#)]
- Liu, J.; He, Y.; Yan, L.; Li, K.; Zhang, C.; Xiang, H.; Li, Y. Nano-sized ZrO₂ derived from metal organic frameworks and their catalytic performance for aromatic synthesis from syngas. *Catal. Sci. Technol.* **2019**, *9*, 2982–2992. [[CrossRef](#)]

18. Zhao, J.-P.; Cao, J.-P.; Wei, F.; He, Z.-M.; Yao, N.-Y.; Feng, X.-B.; Liu, T.-L.; Wang, Z.-Y.; Zhao, X.-Y.; Wei, X.-Y. Catalytic upgrading of lignite pyrolysis volatiles over AlF₃-Modified HZSM-5 to light aromatics: Synergistic effects of one-step dealumination and realumination. *Energy Fuels* **2021**, *35*, 12056–12064. [[CrossRef](#)]
19. Cui, X.; Gao, P.; Li, S.; Yang, C.; Liu, Z.; Wang, H.; Zhong, L.; Sun, Y. Selective production of aromatics directly from carbon dioxide hydrogenation. *ACS Catal.* **2019**, *9*, 3866–3876. [[CrossRef](#)]
20. Santos, V.P.; Pollefeyt, G.; Yancey, D.F.; Sandikci, A.C.; Vanchura, B.; Nieskens, D.L.; de Kok-Kleiberg, M.; Kirilin, A.; Chojecki, A.; Male, A. Direct conversion of syngas to light olefins (C₂-C₃) over a tandem catalyst CrZn-SAPO-34: Tailoring activity and stability by varying the Cr/Zn ratio and calcination temperature. *J. Catal.* **2020**, *381*, 108–120. [[CrossRef](#)]
21. Fu, T.J.; Shao, J.; Li, Z. Catalytic synergy between the low Si/Al ratio Zn/ZSM-5 and high Si/Al ratio HZSM-5 for high-performance methanol conversion to aromatics. *Appl. Catal. B Environ.* **2021**, *291*, 16. [[CrossRef](#)]
22. Song, H.; Laudenschleger, D.; Carey, J.J.; Ruland, H.; Nolan, M.; Muhler, M. Spinel-structured ZnCr₂O₄ with excess Zn is the active ZnO/Cr₂O₃ catalyst for high-temperature methanol synthesis. *ACS Catal.* **2017**, *7*, 7610–7622. [[CrossRef](#)]
23. Wang, Y.; Gao, W.; Wang, K.; Gao, X.; Zhang, B.; Zhao, H.; Ma, Q.; Zhang, P.; Yang, G.; Wu, M.; et al. Boosting the synthesis of value-added aromatics directly from syngas via a Cr₂O₃ and Ga doped zeolite capsule catalyst. *Chem. Sci.* **2021**, *12*, 7786–7792. [[CrossRef](#)]
24. Tripathi, K.; Singh, R.; Pant, K.K. Tailoring the Physicochemical Properties of Mg Promoted Catalysts via One Pot Non-ionic Surfactant Assisted Co-precipitation Route for CO₂ Co-feeding Syngas to Methanol. *Top. Catal.* **2021**, *64*, 395–413. [[CrossRef](#)]
25. van Deelen, T.W.; Mejia, C.H.; de Jong, K.P. Control of metal-support interactions in heterogeneous catalysts to enhance activity and selectivity. *Nat. Catal.* **2019**, *2*, 955–970. [[CrossRef](#)]
26. Liu, C.; Su, J.; Liu, S.; Zhou, H.; Yuan, X.; Ye, Y.; Wang, Y.; Jiao, W.; Zhang, L.; Lu, Y.; et al. Insights into the key factor of zeolite morphology on the selective conversion of syngas to light aromatics over a Cr₂O₃/ZSM-5 catalyst. *ACS Catal.* **2020**, *10*, 15227–15237. [[CrossRef](#)]
27. Yang, J.; Pan, X.; Jiao, F.; Li, J.; Bao, X. Direct conversion of syngas to aromatics. *Chem. Commun.* **2017**, *53*, 11146–11149. [[CrossRef](#)]
28. Nawaz, M.A.; Li, M.; Saif, M.; Song, G.; Wang, Z.; Liu, D. Harnessing the synergistic interplay of Fischer-Tropsch synthesis (Fe-Co) bimetallic oxides in Na-FeMnCo/HZSM-5 composite catalyst for syngas conversion to aromatic hydrocarbons. *Chemcatchem* **2021**, *13*, 1966–1980. [[CrossRef](#)]
29. Dokania, A.; Ramirez, A.; Bavykina, A.; Gascon, J. Heterogeneous Catalysis for the Valorization of CO₂: Role of Bifunctional Processes in the Production of Chemicals. *ACS Energy Lett.* **2019**, *4*, 167–176. [[CrossRef](#)]
30. Liu, C.; Su, J.; Xiao, Y.; Zhou, J.; Liu, S.; Zhou, H.; Ye, Y.; Lu, Y.; Zhang, Y.; Jiao, W.; et al. Constructing directional component distribution in a bifunctional catalyst to boost the tandem reaction of syngas conversion. *Chem Catal.* **2021**, *1*, 896–907. [[CrossRef](#)]
31. Zhou, C.; Shi, J.; Zhou, W.; Cheng, K.; Zhang, Q.; Kang, J.; Wang, Y. Highly Active ZnO–ZrO₂ Aerogels Integrated with H-ZSM-5 for Aromatics Synthesis from Carbon Dioxide. *ACS Catal.* **2019**, *10*, 302–310. [[CrossRef](#)]
32. Li, N.; Jiao, F.; Pan, X.; Chen, Y.; Feng, J.; Li, G.; Bao, X. High-quality gasoline directly from syngas by dual metal oxide-zeolite (OX-ZEO) catalysis. *Angew. Chem. Int. Ed.* **2019**, *58*, 7400–7404. [[CrossRef](#)] [[PubMed](#)]
33. Zhou, W.; Cheng, K.; Kang, J.; Zhou, C.; Subramanian, V.; Zhang, Q.; Wang, Y. New horizon in C1 chemistry: Breaking the selectivity limitation in transformation of syngas and hydrogenation of CO₂ into hydrocarbon chemicals and fuels. *Chem. Soc. Rev.* **2019**, *48*, 3193–3228. [[CrossRef](#)] [[PubMed](#)]
34. Arslan, M.T.; Qureshi, B.A.; Gilani, S.Z.A.; Cai, D.; Ma, Y.; Usman, M.; Chen, X.; Wang, Y.; Wei, F. Single-step conversion of H₂-deficient syngas into high yield of tetramethylbenzene. *ACS Catal.* **2019**, *9*, 2203–2212. [[CrossRef](#)]

Disclaimer/Publisher’s Note: The statements, opinions and data contained in all publications are solely those of the individual author(s) and contributor(s) and not of MDPI and/or the editor(s). MDPI and/or the editor(s) disclaim responsibility for any injury to people or property resulting from any ideas, methods, instructions or products referred to in the content.